applied sciences

MDPI

Article

Modeling the Functioning of the Half-Cells Photovoltaic Module under Partial Shading in the Matlab Package

Mariusz T. Sarniak

Faculty of Civil Engineering, Mechanics and Petrochemistry, Warsaw University of Technology, 09-400 Płock, Poland; mariusz.sarniak@pw.edu.pl

Received: 29 February 2020; Accepted: 3 April 2020; Published: 9 April 2020

check for updates

Abstract: In this paper, the usefulness of photovoltaic modules built of half cells for partially obstructed photovoltaic (PV) installations was analyzed based on verified simulation studies. The parameters of these modules are similar to the classic, but the internal structure is different. Instead of 60 cells in a typical classic PV module, there are twice as many cells in modules with half cells. A simulation model was built in the Matlab/Simulink engineering calculations package, using the "Solar Cell" component, which is a double-diode PV cell replacement model. The simulation model reflects the internal structure of the PV module from half cells so that the output current is divided into two equal parts inside, and the structure of the module is divided into six sections. Simulation tests were performed for the same parameters that were measured during actual measurements of the current–voltage characteristics of the partially shaded PV module. Verification tests were carried out for the photovoltaic module—JAM60S03-320/PR—using the I–V 400 meter. Four different cases of partial shading of the module were verified and one for the case of no shading, but in conditions different from the standard, given by the manufacturer.

Keywords: photovoltaics; partial shading; current–voltage characteristics; photovoltaic module

1. Introduction

Photovoltaics (PVs) are a process of direct conversion of solar radiation into electrical energy [1–4]. The first PV cell was made in 1954 and since then work is underway to improve its construction to increase efficiency, and new materials are being sought. Currently, the vast majority of PV modules produced are built from various types of silicon cells (approximately 90% [5]). However, for silicon, there is an upper theoretical efficiency limit of 29.4% [6]. The latest developments in this area are the construction of a monocrystalline silicon PV cell with a record efficiency of 26.7% [7]. Silicon photovoltaic modules, in which there is a phenomenon of direct conversion of solar energy into electricity, dominate the market and it is estimated that this dominance will last about 10–15 years [5]. However, work is continuing to improve its efficiency, durability, and profitability. The photovoltaic market in Poland has been developing very dynamically recently, and the total installed capacity has already exceeded 1.5 GW [8].

One way to improve performance is to build PV modules from half cells. Due to the double reduction of a single cell in a PV module (by cutting a traditional 156 mm × 156 mm cell in half, a 156 mm × 78 mm cell is created), a new module was built, made of twice as many half-cells. The half-cells are connected in two strings, which eventually are connected in parallel (Figure 1). As a result, such a PV module has similar values of current and output voltage to a typical one. The half-cell module is divided into six sections, protected by bypass diodes (classic modules had three such sections). The result of using half-cell technology is better electrical and mechanical parameters,

resulting in greater energy production. Figure 1a,b shows diagrams of the construction of PV modules of classical construction and made of half-cells, letters A–F are marked with internal division sections, protected by bypass diodes.

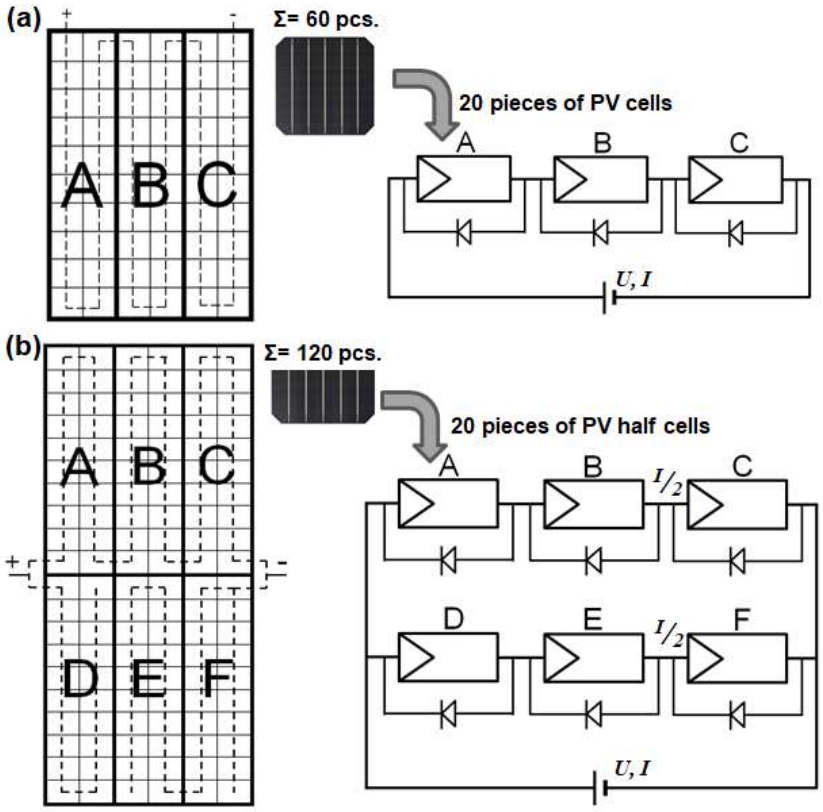

Figure 1. Construction diagram of two types of photovoltaic (PV) modules: (**a**) classic built of 60 whole cells and (**b**) built of 120 half-cells.

Table 1 compares the basic parameters of the module that will undergo simulation tests with a similar one, made in classical technology [9]. The analysis of this comparison may raise some doubts as to the reliability of the previously described advantages of modules made of half cells. From the numerical values in Table 1, you can even draw negative conclusions: larger, heavier, and less efficient with similar electrical parameters. Regardless of the construction of the PV modules, their external characteristics, prepared in shaded conditions, are comparable.

For the operation of classic PV modules under normal conditions (so-called STC—Standard Test Conditions), the Matlab/Simulink (version 2019b, MathWorks, Natick, MA, USA) "Solar Cell" package component was designed and verified [10]. This paper presents only the use of the Matlab/Simulink component "Solar Cell" to simulate partial shading of a module made of half cells. It was not the author's intention to verify the component, because it was developed based on the proven double-diode model of the replacement PV cell. There are various concepts in the literature for modeling PV cells/modules. The most common implementations of surrogate models are single-diode [11,12], double-diode [13,14], and even three-diode [15] models. Modeling uses different calculation methods [16–18]. The purpose of this work is to check the suitability of this component for modeling the functioning of a PV module from half cells in various real environmental conditions. Before adding the "Solar Cell" component to the Matlab/Simulink package, model equations were saved using standard Simulink components or algorithms that were built in the Matlab script language [19–22]. Analyzing the problem of modeling, it often turns out that very complex models do not give better verification. This is the case with the three-diode model [15], which is original but does not significantly increase the accuracy of calculations.

The genesis of the undertaken research was model research for the classic PV module, carried out by the author in work [23]. The proposed method of simulation of partial shading is different from those found in other publications [24–26] and allows quick and easy adaptation to any shading conditions. The issue of shading is also associated with the actual temperature distribution on the surface of PV panels [27,28]. Shaded parts generate an increase in the temperature of PV modules, and in critical situations, this leads to defects in the form of "Hot-Spots".

Table 1. Comparison of parameters of PV modules: standard and half-cell, provided by the manufacturer—in STC. Author's elaboration based on producer data [9].

Name of the PV Module Parameter:	Standard Module JAM60S01-320/PR	Half-Cell Module JAM60S03-320/PR
Type of PV cells	Monocrystalline Silicon	Monocrystalline Silicon
Number of PV cells/half-cells, (pcs.)	60	120
Maximum Power Point—P_{MPP}, (W)	320	320
Open Circuit Voltage—U_{OC}, (V)	40.8	40.22
Voltage in MPP—U_{MPP}, (V)	33.48	33.34
Short Circuit Current—I_{SC}, (A)	10.05	10.16
Current in MPP—I_{MPP}, (A)	9.56	9.6
Module Efficiency—η, (%)	19.6	19.2
Temperature Coefficient of I_{SC}—α_T, (%/°C)	+0.06	+0,051
Temperature Coefficient of U_{OC}—β_T, (%/°C)	−0.30	−0.29
Temperature Coefficient of P_{MPP}—γ_T, (%/°C)	−0.38	−0.36
Temperature in NOCT conditions, (°C)	45	45
Dimensions of PV Module, (mm)	1650 × 991 × 35	1678 × 991 × 35
Mass, (kg)	18.2	18.5

2. Materials and Methods

2.1. Construction of Simulation Model in Matlab Package

Based on the internal structure diagram of the half-cell PV module, which is shown in Figure 1b, a simulation model was designed and implemented in the Matlab/Simulink engineering calculation package using the dedicated solar cell component (Figure 2). This component in the proposed model replaces the half cells, which requires the adoption of half the current intensity for the calculation in relation to the entire cell. In each of the six sections (A÷–F—Figure 1b) of the PV module, a series connection of two "Solar Cell" components has been modeled, which replaces four and sixteen halves of PV cells, respectively, which is indicated in Figure 2 in Section D. The structure of the simulation model corresponds to the accepted methodology of verification tests, in which measurements of current–voltage characteristics at partial shading were planned (Figure 3). For the simulation calculations, the parameters of the PV module from the half-cell model—JAM60S03-320/PR (JA Solar, Beijing, China)—were adopted, which are given in Table 1. Environmental parameters (module temperature and solar radiation intensity) in the simulation model were adopted in the same way as during verification tests (Table 2), during which they were registered by the I–V 400 meter (HT Italia SRL, Faenza, Italy).

In the methodology of simulation tests, a simplifying assumption was adopted, consisting in the fact that a constant temperature value, measured during verification tests in the geometrical center of the reverse part of the PV module, was introduced into the model (in the properties of the solar cell component). The temperature distribution is uneven, but this effect is evident after prolonged shading and during the study (short measurement time) it was not observable. The solar cell component of the Matlab/Simulink package is based on five parameters of the replacement model, determined in STC. This method is simpler than various complicated determination algorithms described in other works [29–31]. The solar cell component is a realization of the double-diode PV substitute model, the developed form of which is shown in Formula (1) and (2). The form of this model is non-linear and

entangled, it can be solved only by means of simulation iterative calculations. The model resulting from the structure of the replacement circuit and its development are as follows [32,33]:

$$I = I_{ph} - I_{d1} - I_{d2} - I_{sh} \tag{1}$$

$$I = I_{ph} - I_{s1}\left[\exp\left(q\frac{U + IR_s}{n_1 k_B T_M}\right) - 1\right] - I_{s2}\left[\exp\left(q\frac{U + IR_s}{n_2 k_B T_M}\right) - 1\right] - \frac{U + IR_s}{R_{sh}} \tag{2}$$

where: I, I_{ph}, I_{d1}, I_{d2}, *and* I_{ph}—mean respectively currents of the cell, photocurrent, diodes, and shunt; U—cell voltage; R_s and R_{sh}—series and shunt resistances; n_1 and n_2—quality factors of the first and second diode; I_{s1} and I_{s2}—saturation currents of the first and second diode; T_M—cell temperature; and q and k_B—electron charge and Boltzmann constant.

In the double-diode model, the diode current component was divided into the diffusion (I_{d1}) and recombination (I_{d2}) part of the so-called dark current of the diode in relation to the simplified single-diode model.

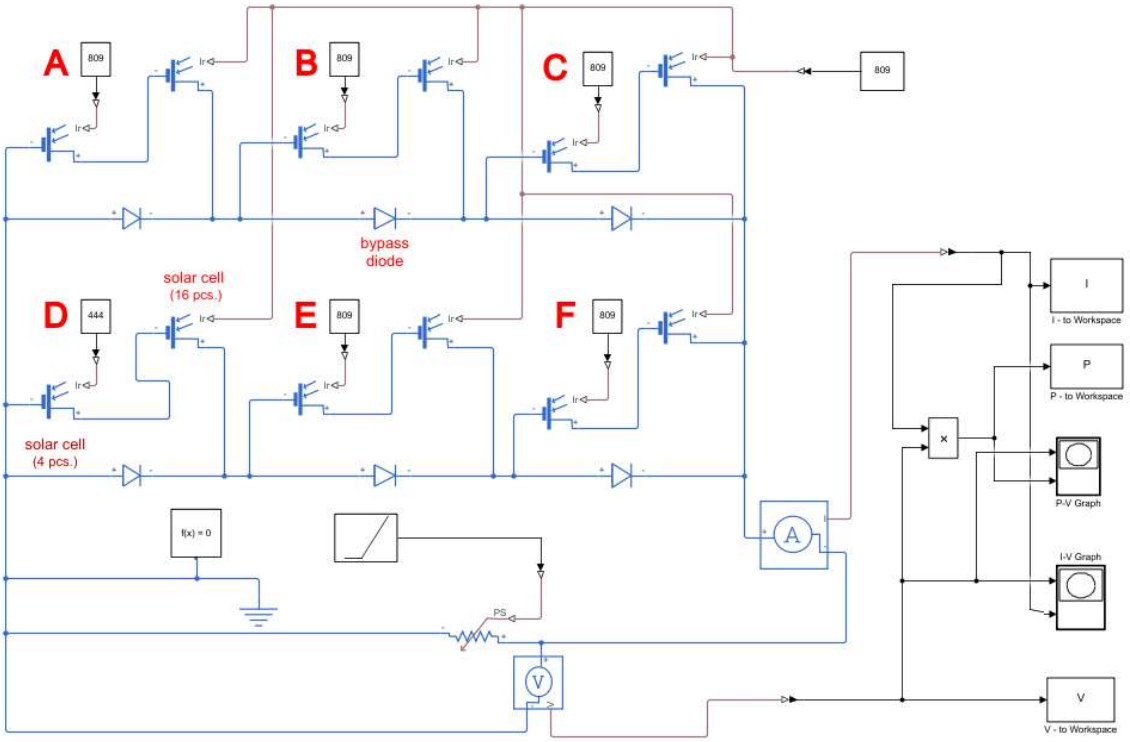

Figure 2. Simulation model of a PV module built from half-cells in the Matlab/Simulink package—the settings shown in the figure apply to measuring point P2 from Table 2 (Section D shading case according to Figure 3a).

2.2. Verification Research Methodology

Verification tests were carried out for the PV module from half cells model, JAM60S03-320/PR, whose fundamental parameters are given in Table 1. Measurements of current–voltage characteristics (in short: I–V) were carried out in accordance with the IEC/PN-EN60891 standard using the dedicated I–V 400 meter [34]. The measurements were made on October 14, 2019 in GPS location: 52.547°N, 19.708°E between 1:00 PM and 2:00 PM. Measurements were carried out under a cloudless sky with a direct solar operation. During the measurements, the average ambient temperature (T_{amb}) was stable at 23 °C and the wind speed was measured at 5 m/s in the north-west direction. The PV module was positioned at an angle of 50° to the horizontal and azimuthally tilted 20° from the south to east. Figure 3 shows the ways and places of partial shading of the tested PV module. The partial shading

effect was achieved by covering part of the PV module surface with a yellow 0.2 mm thick polyethylene film. The screening foil partly transmitted solar radiation to the shaded part of the PV module. Before each measurement, the degree of shading was measured by covering the solar radiation sensor with the I–V 400 meter. The temperature sensor is placed (glued) in the geometrical center of the PV module, on the inside.

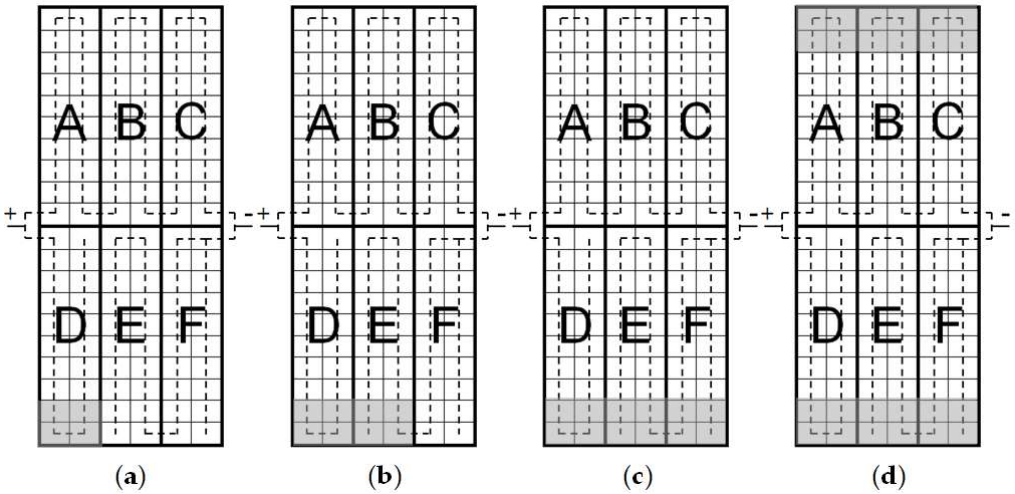

Figure 3. Shading places of the PV module from half cells for the four considered cases verified: (**a**) shading of four halves of PV cells; (**b**) shading of eight halves of PV cells; (**c**) shading of twelve halves of PV cells; and (**d**) shading of twenty-four halves of PV cells.

3. Results

Table 2 presents a summary of the results of verification measurements and provides references to drawing numbers with comparative charts and adopted methods of shading of the tested PV module. The first measuring point P1 (first item in Table 2) was to verify the correctness of the adopted model structure without the shading effect. In the first column of Table 2, reference is made in brackets to drawing numbers with the results of verification tests for all five measuring points P1–P5. The third column of Table 2 gives references to the respective shading case shown in Figure 3, and the last fourth column gives the values of solar radiation intensity that were measured without shading and with partial shading (the last two cases do not concern the measuring point P1).

Table 2. List of parameters and conditions of verification measurements with links to relevant drawing numbers with the results of verification tests.

Measurement Points:	PV Module Temperature T_M, (°C)	Number of Shaded PV Cell Halves (pcs.)	Solar Surface Irradiance Unshaded/Shaded E, (W·m^{-2})
P1 (Figure 4)	35.5	0 [1]	810/0
P2 (Figure 5)	36.9	4 (Figure 3a)	809/444
P3 (Figure 6)	36.2	8 (Figure 3b)	808/443
P4 (Figure 7)	33.5	12 (Figure 3c)	805/442
P5 (Figure 8)	32.8	24 (Figure 3d)	802/432

[1] Measurement without shading.

Figures 4–8 present charts of current–voltage characteristics and power charts for all tested cases of verification tests. The quality of the modules under STC is determined by calculating the fill factor *FF* (3) of the I–V characteristic. In the case of partial shading, such an assessment would be unreliable,

because the I–V characteristics are significantly deformed from the correct ones and the *FF* would be greatly underestimated [32]:

$$FF = \frac{P_{MPP}}{I_{SC}U_{OC}} = \frac{I_{MPP}U_{MPP}}{I_{SC}U_{OC}}, \tag{3}$$

where signs in the Formula (3) are in accordance with that given in Table 1.

There is also a relationship between the fill factor (*FF*) of the I–V characteristic and the efficiency (η) of the PV module according to Formula (4):

$$\eta = \frac{P_{MPP}}{ES} = \frac{I_{MPP}U_{MPP}}{ES} = FF\frac{I_{SC}U_{OC}}{ES}, \tag{4}$$

where the surface area of the PV module (S) is calculated based on the external dimensions (shown in Table 1) and does not take into account the spacing between the halves of the PV cells.

Figure 4 graphically presents the results of the verification of simulation tests in relation to the measurements of the modeled PV module without shadowing.

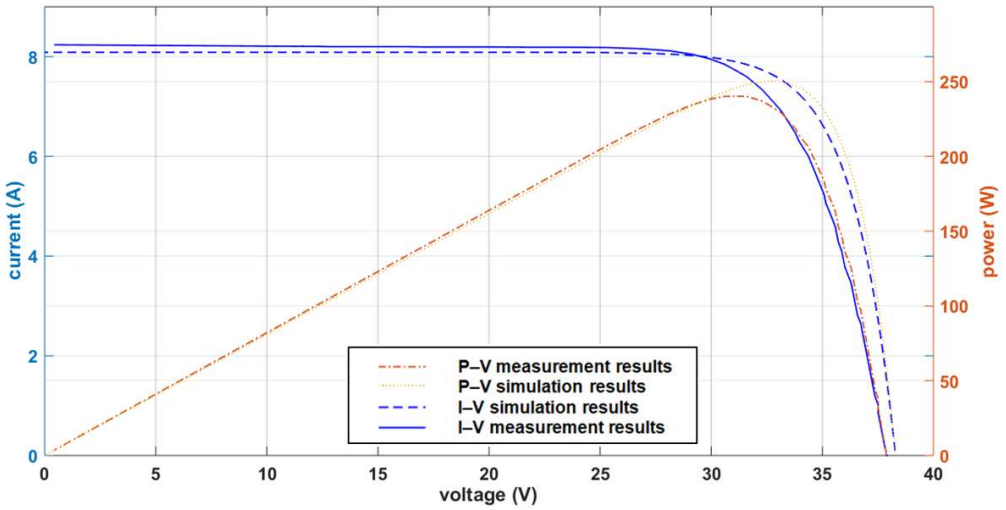

Figure 4. Verification results for measuring point P1 (see Table 2).

In Table 3, relative errors in the comparison of fundamental parameters of I–V characteristics and the values of the *FF* and η coefficients were calculated according to Formulas (3) and (4) for the first measuring point (P1 in Table 2). These calculations determine the accuracy of the method used to model the PV module from half cells, and the maximum relative errors were less than 5%. The comparison of the I–V characteristics in Figure 4 corresponds to the changes resulting from the temperature difference, and therefore this is due to the inaccuracy of the temperatures assumed in the model. The shape of the I–V characteristic made by the I–V 400 meter in relation to the one obtained as a result of the simulation suggests that the temperature was lower during the measurement. For the other measurement points (P2–P5 in Table 2) such calculations would not be correct because there are local extremes on the power graphs (Figures 5–8).

Formulas (5)–(7) [32] allow the calculation of the fundamental parameters of the I–V characteristics of the PV module for a specific temperature T_M in relation to the value at 25 °C (in STC), given by the manufacturer (Table 1). These formulas are based on three temperature coefficients (α_T, β_T, and γ_T) from Table 1:

$$I_{SC}(T_M) = I_{SC}\left[1 + (T_M - 25)\frac{\alpha_T}{100}\right], \tag{5}$$

$$U_{OC}(T_M) = U_{OC}\left[1 + (T_M - 25)\frac{\beta_T}{100}\right], \tag{6}$$

$$P_{MPP}(T_M) = P_{MPP}\left[1 + (T_M - 25)\frac{\gamma_T}{100}\right]. \quad (7)$$

Table 3. Relative errors in the comparison of the basic parameters of the current–voltage (I–V) characteristics and the values of the fill factor (*FF*) and η coefficients for the measuring point P1 graphically shown in Figure 4 (for E = 810 W/m^2, T_M = 35.5 °C, and T_{amb} = 23 °C).

Parameters and Coefficients:	Measurement Results	Simulation Results	Relative Error of Comparison, (%)
I_{SC}, (A)	8.23	8.09	1.7
U_{OC}, (V)	37.87	38.28	1.1
I_{MPP}, (A)	7.61	7.58	0.4
U_{MPP}, (V)	31.58	32.98	4.4
P_{MPP}, (W)	240	250	4
FF, (%)	77.1	80.7	4.7
η, (%)	17.8	18.6	4

Only for the open circuit voltage U_{OC} (Table 4) model was the positive verification of the temperature model obtained (relative error is 3%). Other parameters (I_{SC} and P_{MPP}) calculated according to the models differ significantly in relation to the measurement results. The obtained results of model calculations assumed a simplification in the form of proportionality of the dependence of these three parameters on temperature without taking into account other weather conditions.

Table 4. Comparison of results of calculations of parameters according to models (5), (6), and (7) with the results of measurements for a 35.5 °C PV module temperature.

Parameters:	Model Calculations Results	Measurement Results	Relative Error of Comparison, (%)
I_{SC}, (A)	10.21	8.23	19%
U_{OC}, (V)	39	37.87	3%
P_{MPP}, (W)	307.9	240	22%

Another temperature model [35] makes the value of the module temperature (T_M) dependent on the ambient temperature (T_{amb}) and solar radiation intensity (E) under NOCT (Normal Operating Cell Temperature) conditions, which are more similar to real ones in the considered location of the tests in relation to the STC conditions, represents Formula (8):

$$T_M = T_{amb} + \frac{(NOCT - 20)E}{800}. \quad (8)$$

For the model from Formula (8) a result of 48.3 °C was obtained, which is also much higher than the measured value, which was equal to 35.5 °C. This model assumes NOCT conditions, in which a lower wind speed (1 m/s) is assumed than measured during measurements (5 m/s).

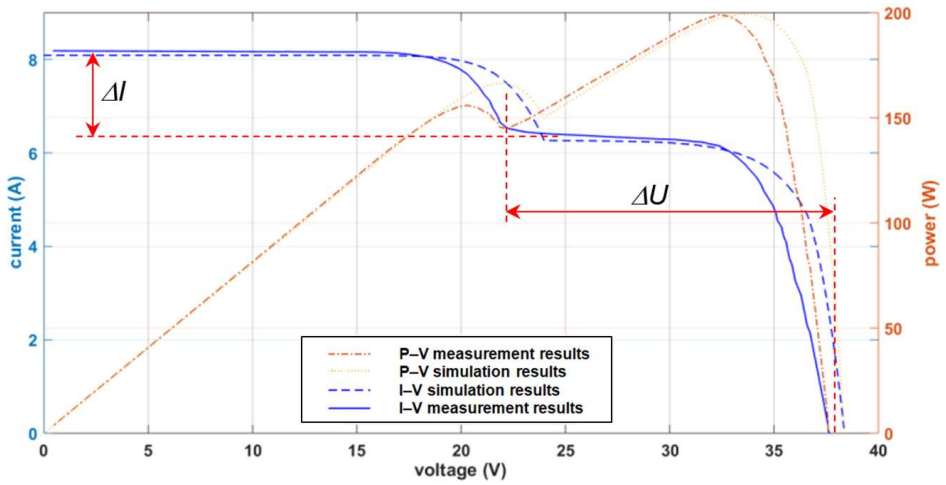

Figure 5. Verification results for measuring point P2 (see Table 2).

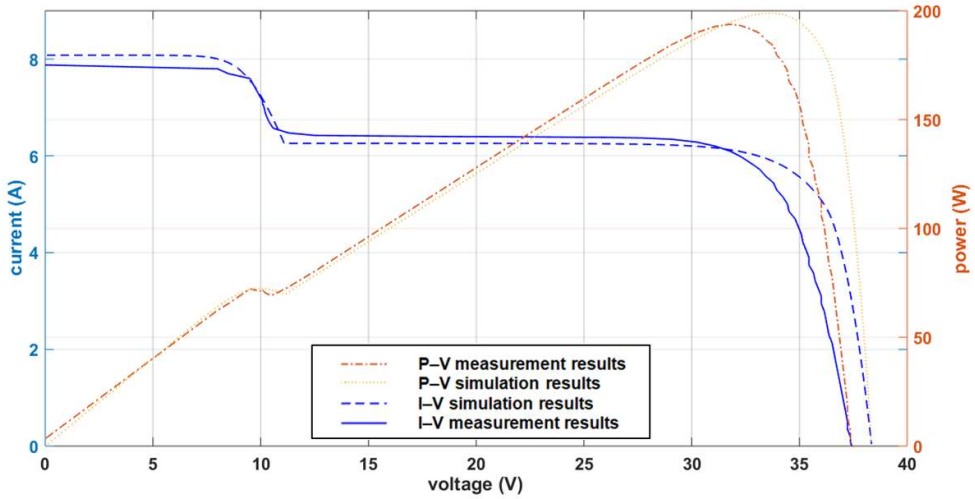

Figure 6. Verification results for measuring point P3 (see Table 2).

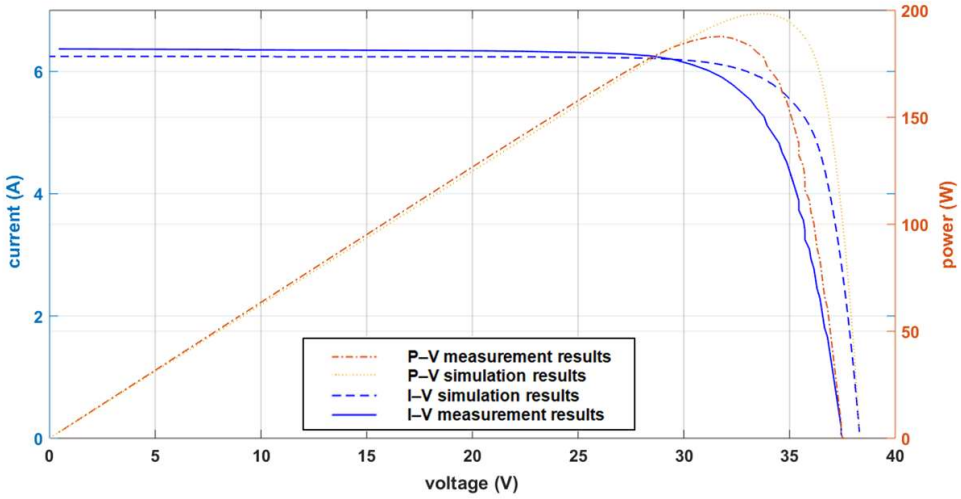

Figure 7. Verification results for measuring point P4 (see Table 2).

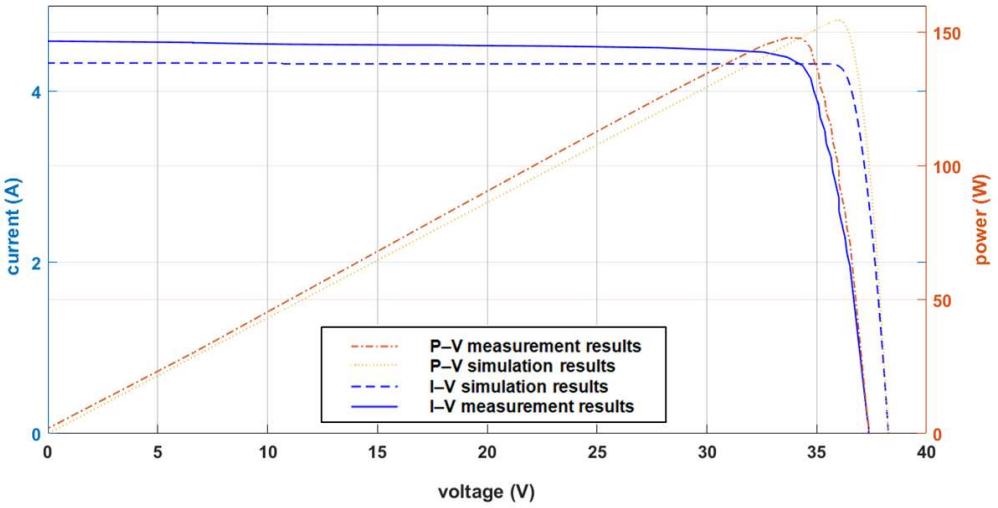

Figure 8. Verification results for measuring point P5 (see Table 2).

Table 5 presented a comparison of the obtained results in relative values with the results of previous studies [23] for two partial shading cases that can be considered as corresponding. It has been assumed that the shading of two whole PV cells corresponds to the shading of four halves of cells, and the shading of four whole PV cells corresponds to eight halves of cells. The interpretation of the adopted average current and voltage decreases is shown in Figure 5. However, this comparison is only indicative due to the different type of module with different peak power and different testing conditions.

Table 5. Comparison of partial shading effects for two monocrystalline silicon PV modules expressed in relative values (made of 60 whole PV cells, based on results from work [23] and 120 half-cells cells—from Table 1).

PV Module Type/Number of Shaded PV Cells	Relative Decrease in Current—$\delta_{\Delta I}$, (%)	Relative Decrease in Voltage—$\delta_{\Delta U}$, (%)
MonoSol 260 EX/2	59	39
JAM60S03-320/PR/4 (Figure 5)	24	42
MonoSol 260 EX/4	61	71
JAM60S03-320/PR/8 (Figure 6)	22	70

4. Discussion and Conclusions

The simulation model proposed in the work was made on the basis of assumed cases of partial shading. The model can be virtually freely modified, e.g., by varying the degree of partial shading for different cells. The author's intention was to build and explain the model accurately for selected cases, but with the possibility of multiple applications for other cases. Temperature parameters are particularly important for the accuracy of the model, which can be varied for individual sections with partial shading and without shading. The model has great application and adaptation possibilities for further research, which should be verified each time with experimental research.

Replacement of PV cells with a double number of their halves in the tested module JAM60S03-320/PR, confirmed the compliance of simulation results with measurements under different conditions from the standard without shading effect (Figure 4). In this case, the tested PV module has I–V characteristics analogous to classic solutions.

A detailed comparative analysis of the results of simulation tests with measurements for the case without shading showed that the potential source of errors is the adoption of constant temperature coefficients under STC in a mathematical model. Additionally, the temperature model for NOCT conditions was not very accurate.

During partial shading of one and two sections of a six-section PV module, a decrease in the current value by approximately 20% was observed per one shaded section, covering approximately 50% (Figure 5) and approximately 75% (Figure 6) the entire measuring range for voltage on a current–voltage characteristic. With the shading of three and all six sections, a decrease in the value of current in the entire voltage measuring range was observed by approximately 40% (Figure 7) and approximately 50% (Figure 8), respectively. The differences in the results of the verification tests result from a simplified temperature measurement method. This hypothesis is confirmed by the shapes of the I–V characteristics. In future studies, consideration should be given to measuring the temperature at several points (depending on the type of shading) or reading from thermographic images. The last two cases resemble the effect of a parallel connection of two classic PV modules with varying degrees of current and voltage mismatch. The obtained results show lower power losses of the PV module made of cell halves resulting from the shading effects compared to the tests carried out for the classic module made of 60 PV cells at work [23], which presents the genesis of this research. The results in relative values of this comparison are given in Table 5. For the two cases compared, more than twice smaller relative current decreases were observed for the module from half-cells.

The PV module built from half-cells is less susceptible to power losses resulting from a specific assembly method. The internal division into six sections, protected by bypass diodes, means that they can be mounted in any way (horizontally or vertically). Reducing the current value by half also causes less power loss due to the lower intensity of heating of this type of module.

In all the cases examined, compliance of the measurement and simulation results was sufficient for practical applications of simulation estimation of the effect of shading on the performance of PV modules made of half cells. There are grounds to suppose that in the future this method will also be able to model the functioning of modules from multiconnector and concentric cells. An important problem in modeling the functioning of PV modules is the dependence of its parameters on temperature. Simplified temperature models do not properly describe the variability of modules parameters throughout the entire operating range.

Funding: This research received no external funding.

Conflicts of Interest: The authors declare no conflict of interest.

References

1. Messenger, R.A.; Ventre, A. *Photovoltaic Systems Engineering*, 4th ed.; CRC Press Taylor & Francis Group: Boca Raton, FL, USA, 2017; ISBN 978-1-4398-0293-9.
2. Conibeer, G.; Willoughby, A. *Solar Cell Materials: Developing Technologies*, 1st ed.; John Wiley & Son: Hoboken, NJ, USA, 2014; ISBN 978-1-118-69581-4.
3. Hegedus, S.; Luque, A. *Handbook of Photovoltaic Science and Engineering*, 2nd ed.; John Wiley & Sons: Hoboken, NJ, USA, 2011; ISBN 978-0-470-72169-8.
4. Kalogirou, S. *McEvoy's Handbook of Photovoltaics: Fundamentals and Applications*, 3rd ed.; Elsevier: London, UK, 2017; ISBN 978-0-12-809921-6.
5. Żdanowicz, T. Photovoltaic system (PV) reception—Procedures and documentation—Part 2. *Magazynfotowoltaika* **2018**, *1*, 16–20. (In Polish)
6. Richter, A.; Hermle, M.; Glunz, S.W. Reassessment of the Limiting Efficiency for Crystalline Silicon Solar Cells. *IEEE J. Photovolt.* **2013**, *3*, 1184–1191. [CrossRef]
7. Green, M.A.; Dunlop, E.D.; Levi, D.H.; Hohl-Ebinger, J.; Yoshita, M.; Ho-Baillie, A.W.Y. Solar cell efficiency tables (version 54). *Prog. Photovolt. Res. Appl.* **2019**, *27*, 565–575. [CrossRef]
8. PSE S.A. Polish Power Grids. Available online: https://www.pse.pl/web/pse-eng (accessed on 1 January 2020).
9. JaSolar Technical Data of the PV Modules. Available online: http://www.jasolar.com/html/en/en_pv/ (accessed on 30 January 2020).
10. Gow, J.A.A.; Manning, C.D. Development of a Photovoltaic Array Model for Use in Power-Electronics Simulation Studies. *IEEE Proc. Electr. Power Appl.* **1999**, *146*, 193–200. [CrossRef]

11. Abbassi, A.; Gammoudi, R.; Ali Dami, M.; Hasnaoui, O.; Jemli, M. An improved single-diode model parameters extraction at different operating conditions with a view to modeling a photovoltaic generator: A comparative study. *Sol. Energy* **2017**, *155*, 478–489. [CrossRef]
12. Yıldıran, N.; Tacer, E. Identification of photovoltaic cell single diode discrete model parameters based on datasheet values. *Sol. Energy* **2016**, *127*, 175–183. [CrossRef]
13. Hassan Hosseini, S.M.; Keymanesh, A.A. Design and construction of photovoltaic simulator based on dual-diode model. *Sol. Energy* **2016**, *137*, 594–607. [CrossRef]
14. Attivissimo, F.; Adamo, F.; Carullo, A.; Lanzolla, A.M.L.; Spertino, F.; Vallan, A. On the performance of the double-diode model in estimating the maximum power point for different photovoltaic technologies. *Measurement* **2013**, *46*, 3549–3559. [CrossRef]
15. Khanna, V.; Das, B.K.; Bisht, D.; Vandana; Singh, P.K. A three diode model for industrial solar cells and estimation of solar cell parameters using PSO algorithm. *Renew. Energy* **2015**, *78*, 105–113. [CrossRef]
16. Gao, X.; Cui, Y.; Hu, J.; Xu, G.; Yu, Y. Lambert W -function based exact representation for double diode model of solar cells: Comparison on fitness and parameter extraction. *Energy Convers. Manag.* **2016**, *127*, 443–460. [CrossRef]
17. Lim, L.H.I.; Ye, Z.; Ye, J.; Yang, D.; Du, H. A Linear Identification of Diode Models from Single I-V Characteristics of PV Panels. *IEEE Trans. Ind. Electron.* **2015**, *62*, 4181–4193. [CrossRef]
18. Obbadi, A.; Errami, Y.; Rmaily, R.; Sahnoun, S.; El, A.; Agunaou, M. Parameters estimation of the single and double diode photovoltaic models using a Gauss—Seidel algorithm and analytical method: A comparative study. *Energy Convers. Manag.* **2017**, *148*, 1041–1054. [CrossRef]
19. Chandani, S.; Anamika, J. Solar Panel Mathematical Modeling Using Simulink. *J. Eng. Res. Appl.* **2014**, *4*, 67–72.
20. Savitha, P.B.; Shashikala, M.S.; Puttabuddhi, K.L. Modelling of 250Wp Photovoltaic Module and Its Performance Analysis Using Matlab /Simulink. *Int. J. Electr. Electron. Data Commun.* **2014**, *2*, 6–12.
21. Tsai, H.-L. Insolation-oriented model of photovoltaic module using Matlab/Simulink. *Sol. Energy* **2010**, *84*, 1318–1326. [CrossRef]
22. Usman, H.; Lawal, S.M.; Shehu, R.S. Behavioral Characteristics of Photovoltaic Cell with Different Irradiation in Matlab/Simuling/Simscape Environment. *Int. Lett. Chem. Phys. Astron.* **2014**, *17*, 316–326. [CrossRef]
23. Sarniak, M.T.; Wernik, J.; Wołosz, K.J. Application of the Double Diode Model of Photovoltaic Cells for Simulation Studies on the Impact of Partial Shading of Silicon Photovoltaic Modules on the Waveforms of Their Current–Voltage Characteristic. *Energies* **2019**, *12*, 2421. [CrossRef]
24. Mohamed, M.A.; Zaki Diab, A.A.; Rezk, H. Partial shading mitigation of PV systems via different meta-heuristic techniques. *Renew. Energy* **2019**, *130*, 1159–1175. [CrossRef]
25. Pendem, S.R.; Mikkili, S. Modelling and performance assessment of PV array topologies under partial shading conditions to mitigate the mismatching power losses. *Sol. Energy* **2018**, *160*, 303–321. [CrossRef]
26. Gallardo-Saavedra, S.; Karlsson, B. Simulation, validation and analysis of shading effects on a PV system. *Sol. Energy* **2018**, *170*, 828–839. [CrossRef]
27. Jaszczur, M.; Teneta, J.; Hassan, Q.; Majewska, E.; Hanus, R. An Experimental and Numerical Investigation of Photovoltaic Module Temperature under Varying Environmental Conditions. *Heat Transf. Eng.* **2019**, 1–14. [CrossRef]
28. Sarniak, M. Influence of Solar Radiation and Ambient Temperature on the Unit Yield of a Photovoltaic System. *Appl. Mech. Mater.* **2015**, *797*, 202–209. [CrossRef]
29. Kang, T.; Yao, J.; Jin, M.; Yang, S.; Duong, T. A Novel Improved Cuckoo Search Algorithm for Parameter Estimation of Photovoltaic (PV) Models. *Energies* **2018**, *11*, 1060. [CrossRef]
30. Toledo, F.J.; Blanes, J.M.; Galiano, V. Two-Step Linear Least-Squares Method For Photovoltaic Single-Diode Model Parameters Extraction. *IEEE Trans. Ind. Electron.* **2018**, *65*, 6301–6308. [CrossRef]
31. Orioli, A.; Di Gangi, A. A procedure to evaluate the seven parameters of the two-diode model for photovoltaic modules. *Renew. Energy* **2019**, *139*, 582–599. [CrossRef]
32. Sarniak, M.T. *Photovoltaic Systems*; Warsaw University of Technology Publishing House: Warsaw, Polish, 2019; ISBN 978-83-7814-926-2. (In Polish)
33. Drabczyk, K.; Panek, P. *Silicon-Based Sollar Cells. Characteristics and Production Processes*; Institute of Metallurgy and Materials Science of Polish Academy of Sciences: Krakow, Polish, 2012; ISBN 978-83-62098-07-1.

34. International Electrotechnical Commission (IEC). *IEC/PN-EN60891 Photovoltaic Devices—Procedures for Temperature and Irradiance Corrections to Measured I-V Characteristics*; IEC: Genewa, Switzerland, 2009.
35. Szymański, B. *Photovoltaic Installations*, 8th ed.; GLOBENERGIA: Kraków, Polish, 2019; ISBN 978-83-65874-00-9. (In Polish)